Nuclear Engineering and Technology 52 (2020) 279–286

Contents lists available at ScienceDirect

Nuclear Engineering and Technology

journal homepage: www.elsevier.com/locate/net

Original Article

Simulating reactive distillation of HIx ($HI-H_2O-I_2$) system in Sulphur-Iodine cycle for hydrogen production

Subhasis Mandal, Amiya K. Jana*

Energy and Process Engineering Laboratory, Department of Chemical Engineering, Indian Institute of Technology, Kharagpur, 721 302, India

ARTICLE INFO

Article history:
Received 10 September 2017
Received in revised form
10 July 2019
Accepted 30 July 2019
Available online 30 July 2019

Keywords:
SI (sulphur-iodine) cycle
HIx system
Reactive distillation
Simulation
Hydrogen production

ABSTRACT

In this article, we develop a reactive distillation (RD) column configuration for the production of hydrogen. This RD column is in the HI decomposition section of the sulphur - iodine (SI) thermochemical cycle, in which HI decomposition and H_2 separation take place simultaneously. The section plays a major role in high hydrogen production efficiency (that depends on reaction conversion and separation efficiency) of the SI cycle. In the column simulation, the rigorous thermodynamic phase equilibrium and reaction kinetic model are used. The tuning parameters involved in phase equilibrium model are dependent on interactive components and system temperature. For kinetic model, parameter values are adopted from the Aspen flowsheet simulator. Interestingly, there is no side reaction (e.g., solvation reaction, electrolyte decomposition and polyiodide formation) considered aiming to make the proposed model simple that leads to a challenging prediction. The process parameters are determined on the basis of optimal hydrogen production as reflux ratio = 0.87, total number of stages = 19 and feeding point at 8th stage. With this, the column operates at a reasonably low pressure (i.e., 8 bar) and produces hydrogen in the distillate with a desired composition (H_2 = 9.18 mol%, H_2O = 88.27 mol% and HI = 2.54 mol%). Finally, the results are compared with other model simulations. It is observed that the proposed scheme leads to consume a reasonably low energy requirement of 327 MJ/kmol of H_2.

1. Introduction

Energy plays a crucial role in socio-economic development of a nation. The International Energy Agency [1] has already projected that the world energy demand will increase by 50% within 2030, 67% of which will be spent in developing and emerging countries. It is a fact that the major portion of energy being used today comes through the carbon-based energy sources, like coal, crude oil etc. Progressive depletion of these fossil fuels reserves and hence rise of oil price as a consequence is a serious threat. Moreover, increasing effect of global warming is another matter of concern. All these factors stimulate a wide-spread research in finding an alternative source of energy [2].

Among various alternatives, hydrogen (H_2) is one of the most promising energy carriers for the future [3–5]. At present, most of the H_2 is produced through thermochemical conversion of fossil fuels [6–8] but this production process emits carbon dioxide (CO_2) to the atmosphere. Today it is widely accepted that a real benefit of CO_2 abatement can only be obtained if H_2 is produced from a non-fossil renewable source.

In order to reduce the emission of CO_2 and the use of fossil fuels, the concerned scientific community is dedicated in exploring the alternative sources of H_2 [9]. One of the prime sources is definitely water, which is quite abundant. H_2 production by decomposition of water can be performed by different ways, namely direct thermal decomposition, electrolysis and thermochemical cycles. Among these techniques, water decomposition through thermochemical cycle processes has received an increasing attention because direct decomposition of water requires very high temperature (about 4000 K) and secures a very low conversion (about 4%) [10]. On the other hand, for a reasonable conversion, the water electrolysis is required to perform at a temperature range of 800–100 °C [11]. However, the thermochemical cycle typically involves low temperature thermal energy, including nuclear or solar energy [12,13].

Water decomposition through thermochemical cycle was first proposed by Funk and Reinstrom [14]. Thermochemical cycles are being studied at various levels of effort since 1970s. However, they have gained large attention since past 20 years, particularly in the United States. Although the thermal efficiency of the

* Corresponding author.
E-mail address: akjana@che.iitkgp.ac.in (A.K. Jana).

https://doi.org/10.1016/j.net.2019.07.033

thermochemical cycle is estimated to be high, versatile technology is needed to be developed to achieve the high efficiency [13]. Keeping this issue in mind, this work aims to produce H_2 through a thermochemical cycle.

Over 100 cycles have been proposed by several research groups. Amongst, Sulphur-Iodine (SI) cycle has shown its promising performance in H_2 production [13]. This thermochemical SI cycle offers several potential advantages. A few of them are as follows [13]:

- All process fluids are recycled and all harmful chemicals are kept in the cycle
- High-temperature (~900 °C) step can be coupled to a nuclear or solar reactor
- Minimal side reactions

The SI cycle has the highest reported efficiency (i.e., 52%) among all the proposed thermochemical cycles based on an integrated flowsheet and thus, in this study, it is adopted for further advancement [13].

The SI thermochemical cycle consists of Bunsen section (Section 1), sulfuric acid (H_2SO_4) decomposition section (Section 2) and hydriodic acid (HI) decomposition section (Section 3). The three reactions of SI cycle are briefly highlighted below.

■ Section 1: Bunsen reaction

$$2H_2O + SO_2 + I_2 \rightarrow H_2SO_4 + 2HI \ (\text{Exothermic, at } 90 - 140oC)$$

■ Section 2: Sulfuric acid decomposition

$$H_2SO_4 \rightarrow H_2O + SO_2 + \frac{1}{2}O_2 \ (\text{Endothermic, at } 750 - 900oC)$$

■ Section 3: Hydriodic acid decomposition [15].

$$2HI \rightarrow H_2 + I_2 \ (\text{Endothermic, at } 100 - 500oC)$$

In Bunsen section, water reacts with iodine and sulfur dioxide exothermally to produce aqueous H_2SO_4 and HI [15]. It is the excess water and iodine that make the liquid-liquid split, that is the conversion of acid mixture into a two-phase solution, a light phase containing sulfuric acid and a heavy phase containing hydrogen iodide and iodine. The latter phase that comprises of HI–H_2O–I_2 is the so-called HIx phase. The H_2SO_4 phase is treated in Section 2, where oxygen is produced through decomposition. On the other hand, the HIx system is dealt with in Section 3, where HI is distilled in a distillation column, and then decomposed to produce hydrogen [9].

General Atomics (GA) claimed that The SI cycle has the potential of producing hydrogen commercially by use of solar and nuclear energy [13]. In the first decade of the 21st century, the SI thermochemical cycle was studied in General Atomics (GA) in collaboration with University of Kentucky (UK) and Sandia National Laboratories (SNL) under the umbrella of the Nuclear Energy Research Initiative (NERI) [13]. However, the interest on this thermochemical cycle is perhaps getting declined, except in India [16] and Japan [17]. This is because of several unresolved issues remained associated with the SI cycle even after researching continuously for 30–40 years. Some of them are as follows:

- Difficulty associated with multiphase reactor design for Bunsen reaction [18].
- Difficulty associated with corrosive environment of HI decomposition section [19,20].

Our current interest focuses on the issues in Section 3. It is widely agreed that Section 3 is one of the most expensive and energy consuming steps of the SI cycle [21]. This Section 3 has a couple of problems [21] as listed below:

- HI decomposition is an equilibrium limited reaction and maximum possible conversion is 22.4% at 723 K.
- Azeotropic composition of HI in distillate in the HI distillation column is 13 mol% and it corresponds to a large energy requirement to evaporate the water in excess.

In order to overcome these problems, several alternatives have been proposed, including an electro-electrodialysis HI concentration process [22] and an I_2 extraction process with phosphoric acid (H_3PO_4). These apart, there is another interesting scheme, namely reactive distillation (RD) [21] that allows the simultaneous HI decomposition reaction and H_2 separation in a single unit. It also takes care of the issues concerning chemical equilibrium limited reaction and azeotrope formation [23]. Among all these schemes, RD has emerged as a strong candidate. With this, H_2 yield increases by shifting the HI decomposition reaction equilibrium to product side by removing H_2 from reaction field. H_2 production from thermochemical SI cycle via RD column has been studied by several groups, namely Belaissaoui et al. [21], Roth and Knoche [24], Goldstein et al. [25] and Murphy and O'Connell [26].

To develop the RD column, we need accurate phase equilibrium as well as reaction kinetics. Here, we adopt a simple kinetic model inbuilt in Aspen Plus flowsheet simulator and the Soave-Redlich-Kwong (SRK) based homogeneous (ϕ-ϕ) thermodynamic model. This vapour liquid equilibrium model is developed in our earlier study [27], and tested comparing with experimental data and a latest model of Murphy and O'Connell [26]. It is interesting to note that the proposed RD model disregards all side reactions, such as solvation reaction, electrolyte decomposition and polyiodide formation, making it simple but more challenging. Finally, a systematic comparison is made between the proposed and the existing RD column configurations.

2. Modelling of reactive distillation

In the present study, an RD column is developed to use for simultaneous reaction and multicomponent separation. The following assumptions are adopted in modelling the RD column [28]:

- Tray vapour holdups are neglected
- Liquid holdup varies in each tray
- All trays are perfectly mixed
- Column is perfectly insulated (thermally)
- Algebraic correlations are used to compute the phase enthalpies
- Fast energy dynamics is supposed (i.e., the energy accumulation in the trays is neglected)
- Nonideality exists in both liquid and vapour phase

The scheme of a typical nth plate is shown in Fig. 1. The tray receives a liquid feed mixture. Side streams are withdrawn from the same tray. The model consisting of MESH equations is presented below [28].

Total mole bxalance

$$\frac{dm_n}{dt} = L_{n-1} + V_{n+1} + F_n - \left(L_n + S_n^L\right) - \left(V_n + S_n^V\right) + R_f \sum_{i=1}^{n} \delta_i r_n \varepsilon_n \quad (1)$$

Component mole balance

$$\frac{d(m_n x_{n,i})}{dt} = L_{n-1}x_{n-1,\,i} + V_{n+1}y_{n+1,\,i} + F_n z_{n,\,i} - \left(L_n + S_n^L\right)x_{n,\,i} - \left(V_n + S_n^V\right)y_{n,\,i} + R_f \delta_i r_n \varepsilon_n \tag{2}$$

Energy balance

$$\frac{d\left(m_n H_n^L\right)}{dt} = L_{n-1}H_{n-1}^L + V_{n+1}H_{n+1}^V + F_n H_n^F - \left(L_n + S_n^L\right)H_n^L - \left(V_n + S_n^V\right)H_n^V + R_f r_n H_n^r \varepsilon_n - Q_n \tag{3}$$

Equilibrium

$$y_{n,\,i} = k_{n,\,i}x_{n,\,i} \tag{4}$$

with

$$k_{n,\,i} = \frac{\varphi_{n,\,i}^L}{\varphi_{n,\,i}^V} \tag{5}$$

Summation

$$\sum_{i=1}^{N_C} x_{n,\,i} = 1 \tag{6}$$

$$\sum_{i=1}^{N_C} y_{n,\,i} = 1 \tag{7}$$

It should be noted that there is no side cut involved in the RD column [28]. The heat loss (Q_n) is neglected under the assumption that the RD column is perfectly insulated.

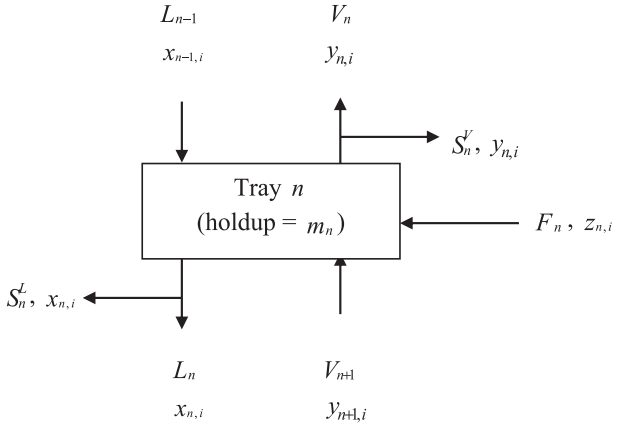

Fig. 1. Quantities associated with a typical nth tray.

2.1. Vapour liquid equilibrium (VLE) model

The VLE for the HIx system developed in our earlier work [27] is briefly presented below. At equilibrium, we have the following relationship considered for a typical species i distributed among multiple phases [26] as:

$$f_i^V = f_i^L = f_i^S \tag{8}$$

Homogeneous approach (ϕ-ϕ).

In this approach, the vapour and liquid phase fugacities are calculated by the equation of state (EoS) model. In this work, we employ the SRK EoS model for the HIx system with:

$$f_i^V = y_i\varphi_i^V(T,P,y)P \tag{9}$$

$$f_i^L = x_i\varphi_i^L(T,P,x)P \tag{10}$$

The standard thermodynamic relation for fugacity coefficient is given [29,30] as:

$$\ln\varphi = \int_0^P (Z-1)\frac{dp}{p} \tag{11}$$

Obtaining an expression for $(Z-1)$ term for the above equation from an EoS model (i.e., SRK) and integrating, one obtains the following expression:

$$\ln\left(\varphi_i^{\omega}\right) = \frac{B_i}{B_\omega}(Z_\omega - 1) - \frac{A_\omega^2}{B_\omega}\left(\frac{2\overline{A_{\omega i}^2}}{A_\omega^2} - \frac{B_i}{B_\omega}\right)\ln\left(\frac{Z_\omega + B_\omega P}{Z_\omega}\right) - \ln(Z_\omega - B_\omega P) \tag{12}$$

All the relevant terms specific to the SRK are defined in Table 1. The relationship between these parameters and SRK are provided

Table 1
Parameters in Equation (12).

Parameter	SRK
θ^{ω}	$\frac{B_i}{B_\omega}$
η^{ω}	$\frac{A_\omega^2}{B_\omega}\left(\frac{2\overline{A_{\omega i}^2}}{A_\omega^2} - \frac{B_i}{B_\omega}\right)$
λ_1^{ω}	$B_\omega P$
λ_2^{ω}	0
ρ^{ω}	$B_\omega P$

in Ref. [31].

The compressibility factor is computed by a cubic form of equation under an EoS model. For the SRK model, it has the following form:

$$Z_\omega{}^3 - Z_\omega{}^2 + \left[A_\omega{}^2 P - B_\omega P(1 + B_\omega P)\right] Z_\omega - A_\omega{}^2 P B_\omega P = 0 \tag{13}$$

This equation has three roots and the first root can easily be determined by the use of a numerical convergence method (e.g., Newton-Raphson approach). The rest two roots can be determined subsequently from the quadratic form of Equation (13). It should be noted that the largest real root corresponds to the vapour phase and the smallest real root to the liquid phase [32]. There is no physical significance for the intermediate real root. Again, when there exists only one real root with $T < T_C$, it corresponds to the vapour phase if the corresponding density is lower than the critical density ($\rho < \rho_C$) and to the liquid phase if $\rho > \rho_C$. When $T > T_C$, the single real root corresponds to the vapour phase.

For a multicomponent system, the mixing rule is taken into account. In the equation of state (EoS) model,

$$a_i = 0.42747 \frac{R^2 T_{ci}^2}{P_{ci}} \tag{14}$$

$$b_i = 0.08664 \frac{R\, T_{ci}}{P_{ci}} \tag{15}$$

$$A_L = \left[\sum_{i=1}^{N_c}\sum_{j=1}^{N_C} x_i x_j A_i A_j \left(1 - p_{ij}\right)\right]^{\frac{1}{2}} \tag{16}$$

$$A_i = \frac{a_i^{0.5} \alpha_i^{0.5}}{RT} \tag{17}$$

$$\alpha_i = \left[1 + \left(0.48508 + 1.5517 v_i - 0.1561 v_i^2\right)\left(1 - \sqrt{T_{ri}}\right)\right] \tag{18}$$

$$T_{ri} = \frac{T}{T_{Ci}} \tag{19}$$

$$l_{ij} = l_{a_{ij}} + l_{b_{ij}} T + \frac{l_{c_{ij}}}{T} \tag{20}$$

$$l_{ij} \neq l_{ji} \tag{21}$$

$$B_L = \sum_{i=1}^{N_c} x_i B_i \tag{22}$$

$$B_i = \frac{b_i}{RT} \tag{23}$$

$$A_V = \left[\sum_{i=1}^{N_c}\sum_{j=1}^{N_C} y_i y_j A_i A_j \left(1 - p_{ij}\right)\right]^{\frac{1}{2}} \tag{24}$$

$$B_V = \sum_{i=1}^{N_C} y_i B_i \tag{25}$$

$$\overline{A_{Vi}} = \left[A_i \sum_{j=1}^{N_c} y_j A_j \left(1 - p_{ij}\right)\right]^{\frac{1}{2}} \tag{26}$$

$$p_{ij} = p_{a_{ij}} + p_{b_{ij}} T + \frac{p_{c_{ij}}}{T} \tag{27}$$

$$p_{ij} = p_{ji} \tag{28}$$

The binary interaction parameters, l_{ij} and p_{ij} are defined in Equations (20) and (27), respectively. These parameters are regressed using the Aspen Plus flowsheet simulator. Basically, they are obtained using the maximum likelihood method implemented in the said simulator and are reported in Table 2 (T in °C). Moreover, values of the Pitzer acentric factor, υ are taken from Ref. [32].

2.2. Reaction equilibrium

As stated, the kinetic model available in the Aspen Plus is used in the process simulation. The reaction equilibrium constant of HI decomposition, K^{eq} is a function of temperature and is defined by the following form:

$$\ln K^{eq} = A' + \frac{B'}{T} + C' \ln(T) + D'T \tag{29}$$

where, T is in K. Parameters for the above equation is taken from the Aspen Plus [33] as: $A' = -2.326$, $B' = -1233.57$, $C' = 0$ and $D' = 0$.

It should be noted that the following correlation can be used in the process model defined in Eq. (1) – (7) to compute the term associated with the reaction.

$$\overline{C}_{HI} = \left(\frac{\overline{C}_{H_2}\overline{C}_{I_2}}{K^{eq}}\right)^{0.5} \tag{30}$$

Here, the reaction equilibrium model disregards all side reactions, among which, the solvation reaction, electrolyte decomposition and polyiodide formation are quite common.

3. Simulation results

A reactive distillation column represents Section 3 of the SI thermochemical cycle. A feed stream, consisting of HI, H_2O and I_2, enters the RD column, in which, both reaction (i.e., HI decomposition) and separation of H_2 in the quaternary mixture ($HI–H_2O–I_2–H_2$) take place. This leads to improve the yield of hydrogen.

Table 2
The SRK binary interaction parameters for vapour and liquid phase.

Component *i*	H_2O	H_2O	HI
Component *j*	HI	I_2	I_2
Vapour phase			
	0.371394	→2.24553	→1.1908
	→ 4.82E-03	3.30E-03	→ 1.98E-03
	500.0137	231.9136	→ 169.965
Liquid phase			
	→ 42.5703	1.513953	1.79018
	0.201085	→ 1.3737	6.768968
	0.103122	−0.02933	−0.025
	→ 1.41E-03	7.64E-03	0.011331
	→ 9183.94	3558.189	690.4659
	238.6987	→ 1372.75	→ 3765.99

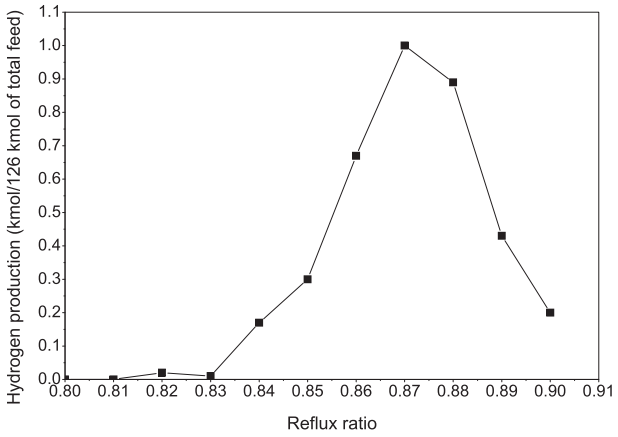

Fig. 2. Effect of reflux ratio on hydrogen production (total number of stages (n_T) = 19 and feeding point at 8th tray).

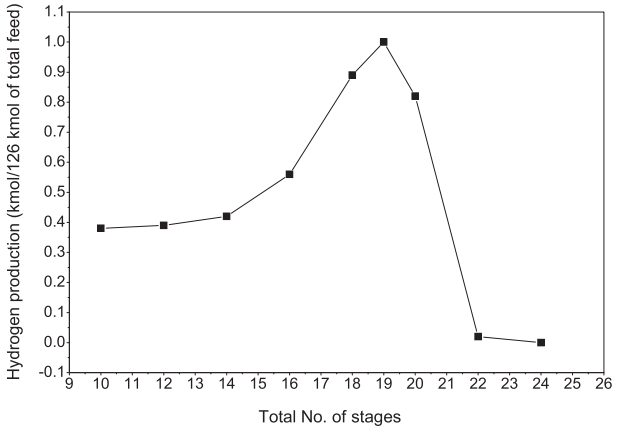

Fig. 3. Effect of total number of stages on hydrogen production (reflux ratio = 0.87 and feeding point at the middle of the column for all n_T).

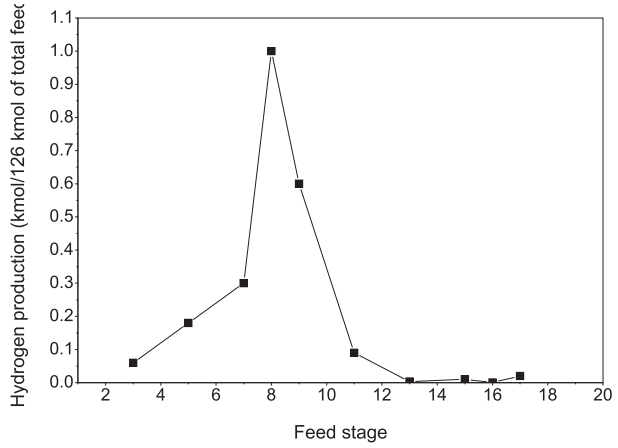

Fig. 4. Effect of feed stage (F) on hydrogen production (reflux ratio = 0.87 and total number of stages = 19).

As shown in Fig. 5, the ternary liquid feed (51 mol% H_2O, 10 mol% HI and 39 mol% I_2) to the RD column that is basically discharged from the acid separator at 120 °C and 1.85 bar is heated to 140 °C and then pumped to the feed tray (i.e., 8th tray) at 8 bar with a flow rate of 126 kmol/h. This feed condition is maintained to favor the reaction with separation in the RD column.

3.1. Parametric study

For the developed RD column, we need to choose the reflux ratio (RR), total number of stages (n_T) and feed location. A sensitivity analysis is conducted below to select these parameters to attain optimal hydrogen production. It should be noted that initial values of these parameters are adopted from the Aspen Plus simulator.

Fig. 2 demonstrates the effect of reflux ratio on the production of hydrogen. In this simulation experiment, reflux is varied keeping other parameters values fixed (i.e., $n_T = 19$ and feeding point at 8th tray). The operation pressure is set at 8 bar. With this, we produce the plot between hydrogen production (in kmol/126 kmol feed) vs. reflux ratio and it becomes obvious that the maximum hydrogen production is achieved at RR of 0.87.

In the next phase, we attempt to select the total number of stages (n_T) keeping the reflux ratio fixed at 0.87, pressure at 8 bar and feeding point at the middle of the column for all n_T. The influence of n_T on the hydrogen production is depicted in Fig. 3. At the existing condition, the best performance is observed with n_T equals 19.

Finally, Fig. 4 illustrates how the feed location affects the hydrogen production. For this simulation experiment, the reflux ratio, pressure and n_T are kept constant at 0.87, 8 bar and 19, respectively. It is evident that the feeding location at 8th stage leads to the maximum hydrogen production. Accordingly, we select RR = 0.87, $n_T = 19$ and feeding point at 8th stage for the subsequent study.

3.2. Column profile

As stated, the proposed RD column operated at 8 bar produces H_2 in vapour phase. Since HI decomposes to H_2 and I_2, a total of 4 components, namely H_2, HI, H_2O, I_2, participate in separation in the RD column. Among them, H_2 has the lowest boiling point (i.e., −252.87 °C at 1 atm) and I_2 has the highest boiling point (i.e., 184.3 °C at 1 atm). As a consequence, the entire amount of H_2 comes out with the distillate stream and that of I_2 gets discharged with the bottoms. It is evident in Fig. 5 that the two intermediate components, namely HI (boiling point at 1 atm = 34 °C) and H_2O (boiling point at 1 atm = 100 °C) are present in both the distillate and bottom streams.

Fig. 6 depicts the temperature profile of the simulated RD column. In the rectifying section (i.e., Tray 1–7) of the column, the HI decomposition mostly occurs. This is because the rectifying section has low iodine content, and for this, according to the Le Chatelier's principle, the reaction (endothermic) equilibrium shifts towards the production of hydrogen, the least boiling component. Because of cooling at the condenser the temperature at the top section is reasonably low. Then gradually the temperature rises toward the bottom and it expectedly reaches the highest value (i.e., 178.32 °C) in the reboiler where boiling occurs.

Fig. 7 displays the variation of phase composition of HI, H_2O and I_2 against the distillation stage. In Fig. 7A, the H_2 production profile is also included. As indicated, the top of the RD column is enriched with H_2 and bottom with I_2. Other two intermediate components, namely H_2O and unconverted HI are present in both the top and bottom products. Actually, as feed enters 8th stage, the heaviest component, I_2 moves down and thus, its composition increases from 9th stage onward to the reboiler (see Fig. 7B). On the other hand, the light component, HI starts accumulating in the top section of the RD column where HI decomposition occurs.

3.3. A comparative study

Table 3 compares the proposed column with different RD

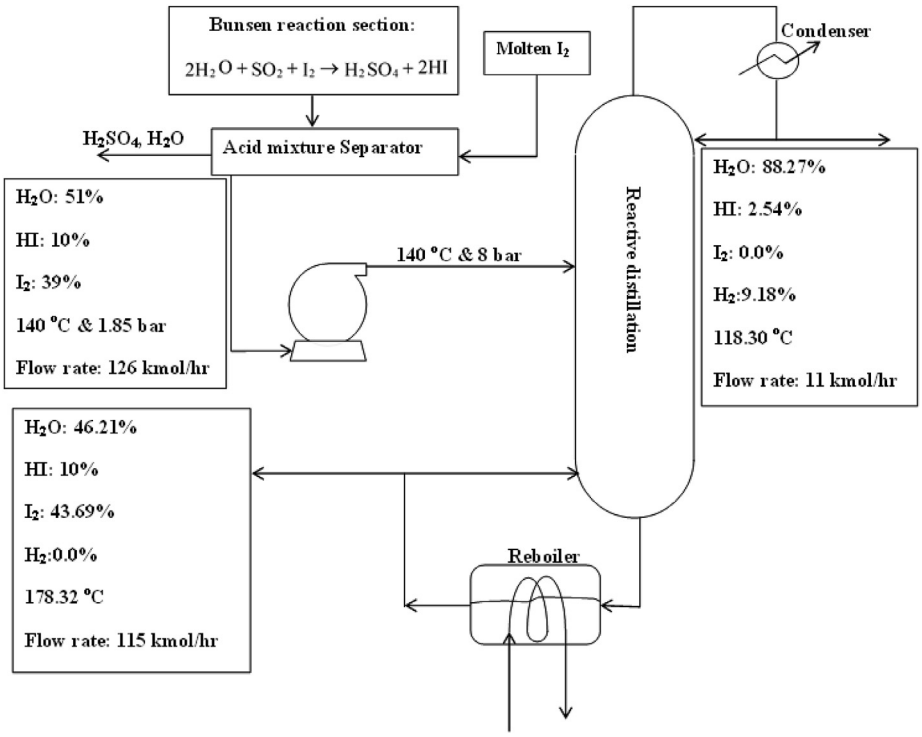

Fig. 5. Schematic diagram of the overall reactive distillation process for the HIx system.

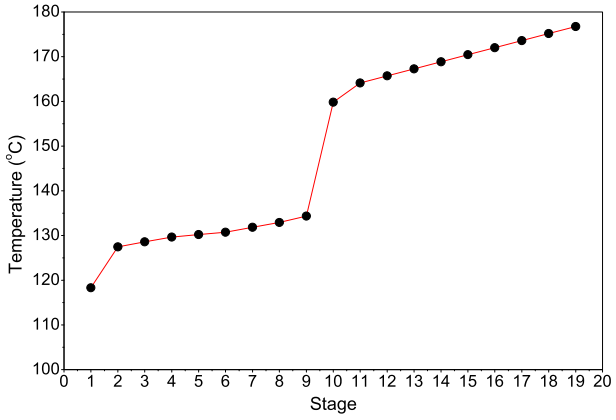

Fig. 6. Temperature profile of the reactive distillation column for quaternary HIx system.

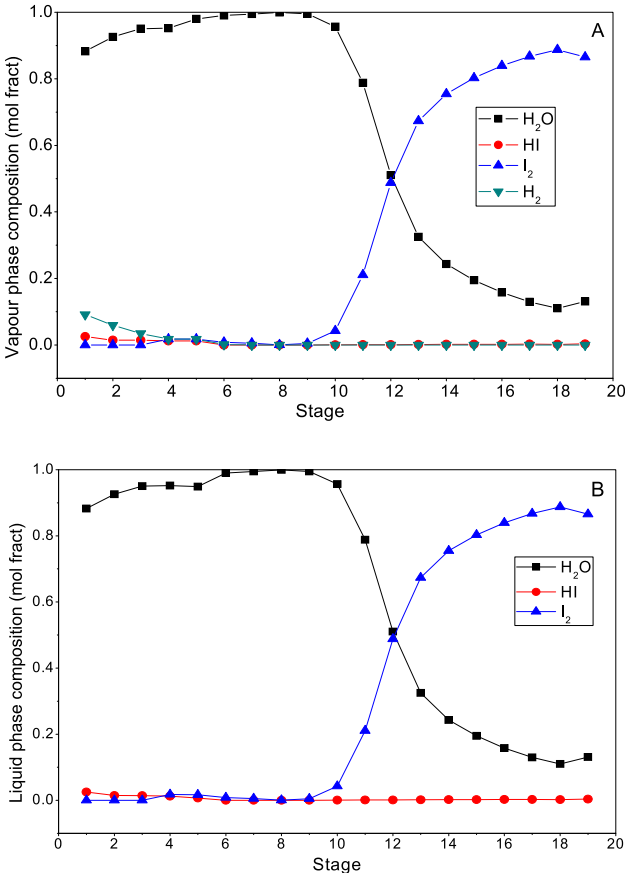

Fig. 7. Composition profile of the reactive distillation column: (A) vapour composition vs. stage, and (B) liquid composition vs. stage.

schemes. As shown, Goldstein et al. [25], Belaissaoui et al. [21], and Roth and Knoche [24] have considered high operating pressure (i.e., 50, 22 and 22 bar, respectively) as well as bottom temperature (i.e., 316, 338.94 and 310 °C, respectively) in RD operation to produce hydrogen. On the other hand, the RD column of Murphy and O'Connell [29], and the proposed one operate with relatively low pressure (i.e., 12 and 8 bar, respectively) as well as bottom temperature (i.e., 232 and 178.62 °C, respectively). Also, there is a variation in the total number of trays, reflux ratio and the VLE model used. The proposed column shows a competitive performance with that of Murphy and O'Connell [29] in the aspect of required feed for producing 1 kmol of H_2. On this point, Roth and Knoche [24] have also reported the same value. It is a fact that depending on the reaction conversion and separation efficiency, the feed rate and heat requirement vary for producing 1 kmol of H_2. With this, the energy requirement for 1 kmol of H_2 production is

Table 3
A comparative study of RD columnsof the HIx system.

RD column operating conditions	Reference				
Item	Roth and Knoche [24]	Belaissaoui et al. [21]	Goldstein et al. [25]	Murphy and O'Connell [29]	Proposed model
Feed composition (mol%)	H_2O- 51% HI- 10% I_2- 39%	H_2O- 51% HI- 10% I_2- 39%	H_2O- 51% HI- 10% I_2- 39%	H_2O- 51% HI- 10% I_2- 39%	H_2O- 51% HI- 10% I_2- 39%
Distillate composition (mol%)	H_2O-54% HI-16% H_2-30% (RD-only)	H_2O-91.036% HI-0.002% H_2-8.962% (RD-only)	H_2O-68.49% HI-0.28% H_2-23.11% I_2-8.12% (RD followed by separator)	H_2O-32.4% HI-0.0% H_2-63.3% I_2-4.3% (RD flowsheet)	H_2O-88.27% HI-2.54% H_2-9.18% (RD-only)
Feed temperature (°C)	262	259.78	311	227	140
Feed Pressure (bar)	–	–	50	–	8
No of stages[a]	–	11	25	10–13	19
Feed type	Saturated liquid	Saturated liquid	–	–	Subcooled liquid
Feed stage	–	10	18	9	8
Operating pressure (bar)	22	22	50	12	8
Top temperature (°C)	221	213	275.4	215	118.3
Bottom temperature (°C)	310	338.94	316	232	178.62
Feed rate (kmol/hr) to produce 1 kmol of H_2/hr	126	22.52	41.6	126 to 140	126
VLE model	–	Neumann's proposed model	Neumann's proposed model	Murphy and O'Connell's proposed model	SRK with a proposed parameter set
Reflux ratio	–	5	–	0.75	0.87
Energy requirement (MJ/kmol H_2)		–			327
	237 (heat integrated scheme)		375 (heat integrated scheme)	367 (heat integrated scheme)	(RD-only)

[a] Including condenser and reboiler – Not available.

lowest for the heat integrated RD (HIRD) column of Roth and Knoche (i.e., 237 MJ) followed by the proposed RD-only (i.e., 327 MJ), and HIRD of Murphy and O'Connell (i.e., 367 MJ) and Goldstein et al. (i.e., 375 MJ). As indicated, all the schemes compared in Table 3 (except the proposed one) consider heat integration with the RD column.

4. Conclusion

In this work, we formulate a reactive distillation column for the HIx system of SI thermochemical cycle for the production of hydrogen. Developing a fundamental process model with disregarding all side reactions, we simulate the column using a homogeneous phase equilibrium model that considers the nonideality in both the liquid and vapour phase, and a HI decomposition kinetic model. The column parameters (RR = 0.87, $n_T = 19$ and feeding point at 8th stage) are determined through the sensitivity analysis. With this, we perform a systematic comparison between the proposed column and the existing ones. It is observed that the proposed RD shows a competitive result, particularly in terms of H_2 production, with the simulation results reported by Murphy and O'Connell [29], and Roth and Knoche [24].

Acknowledgement

Financial support for this work by the Bhabha Atomic Research Centre (BARC), India, Grant 2009/36/97-BRNS/3228 is gratefully acknowledged.

Nomenclature

Abbreviation

EoS	Equation of state
HIRD	heat integrated RD
HIx	A system consisting of HI–H2O–I2
MESH	Material balance, vapour-liquid Equilibrium, mole fraction Summation and Heat balance
RD	Reactive distillation
RR	Reflux ratio (dimensionless)
SI	Sulphur-Iodine cycle
SRK	Soave-Redlich-Kwong (EoS)
VLE	Vapour liquid equilibrium

Symbol

A'	B', C', D' Coefficients in reaction equilibrium Equation (29) (dimensionless)
A,C	Coefficients in phase equilibrium (dimensionless)
a_i	EoS model coefficient pressure correction factor [bar.(liter/mol)2]
B	Coefficients in phase equilibrium (K)
b_i	EoS model coefficient volume correction factor (liter/mol)
D	Coefficients in phase equilibrium (K-1)
$\overline{C}$	Mass concentration (kg/m3)
f	Fugacity (bar)
k	Feed flow rate (kmol/hr)
H^L	Liquid enthalpy (J/kmol)
k	Vapour-liquid equilibrium coefficient (dimensionless)
K^{eq}	Reaction equilibrium constant (dimensionless)

l_{ij}	Binary interaction parameter
L	Liquid flow rate (kmol/hr)
m	Liquid hold up (kmol)
N_C	Total number of components (dimensionless)
n_T	Total number of stages (dimensionless)
p_{ij}	Binary interaction parameter
P	Pressure (bar)
P_C	Critical pressure (bar)
P_r	Reduced pressure (dimensionless)
p_{ij}	Binary interaction parameter for pair *i-j* (dimensionless)
Q	Heat loss (kW)
R_f	Multiplication factor (zero for nonreactive and one for reactive stage)
r_n	Reaction rate (kmol/m3 hr)
R	Universal gas constant (8.314 J/mol K)
k	Side stream flow rate (kmol/hr)
T	Temperature (0C or K)
T_C	Critical temperature (0C)
T_r	Reduced temperature (dimensionless)
υ	Pitzer factor (dimensionless)
V	Vapour flow rate (kmol/hr)
x	Liquid phase composition (mole fraction)
y	Vapour phase composition (mole fraction)
Z	Compressibility factor (dimensionless)
z	Feed composition (mole fraction)
δ	Stoichiometric coefficient (dimensionless)
ε	Volume of catalyst (m3)
α	EoS model coefficient (dimensionless)
φ	Fugacity coefficient (dimensionless)

Suffix

i	Component index
j	Component index (when interaction involved)
L	Liquid
n	Tray index
S	Solid
V	Vapour
ω	Phase index (for liquid, $\omega = L$ and for vapour, $\omega = V$)

References

[1] IEA (International Energy Agency), World Energy Outlook 2006, OECD/IEA, Paris, 2006.

[2] X. Yan, Y. Tachibana, H. Ohashi, H. Sato, Y. Tazawa, K. Kunitomi, A small modular reactor design for multiple energy applications: HTR50S, Nucl. Eng. Technol. 45 (2013) (2013) 401–414.

[3] J.S. Choi, Y.J. Shin, K.Y. Lee, J.H. Choi, Two-dimensional simulation of hydrogen iodide decomposition reaction using fluent code for hydrogen production using nuclear technology, Nucl. Eng. Technol. 47 (2015) 424–433.

[4] Z. Chen, S.S.E.H. Elnashaie, Bifurcation behaviour during the hydrogen production in two compatible configurations of a novel circulating fluidized bed membrane reformer, Chem. Eng. Res. Des. 83 (2005) 679–685.

[5] R.F. Susanti, L.W. Dianningrum, T. Yum, Y. Kim, Y.W. Lee, J. Kim, High yield hydrogen production by supercritical water gasification of various feedbacks: alcohols, glucose, glycerol and long – chain alkanes, Chem. Eng. Res. Des. 92 (2014) 1834–1844.

[6] J.S. Choi, Y.J. Shin, K.Y. Lee, Y.S. Yun, J.H. Choi, Pump design and computational fluid dynamic analysis for high temperature sulfuric acid transfer system, Nucl. Eng. Technol. 46 (2014) 363–372.

[7] M. Balat, M. Balat, Political, economic and environmental impacts of biomass-based hydrogen, Int. J. Hydrogen Energy 34 (2009) 3589–3603.

[8] W. Wukovits, W. Schnitzhofer, K. Urbaniec, Process routes of hydrogen production from fossil and renewable resources, in: D.R. Honnery, P. Moriarty (Eds.), Hydrogen Production: Prospects and Processes, Nova Science Publishers, Hauppage, 2012, ISBN 978-1-62100-285-7, pp. 43–93.

[9] S.T. Revankar, N.R. Brown, C. Kane, S. Oh, Development of Efficient Flowsheet and Transient Modeling for Nuclear Heat Coupled Sulfur Iodine Cycle for Hydrogen Production, Project No. 06-060, Award No. DE-FC07-06ID14749, 2010.

[10] S.Z. Baykara, Experimental solar water thermolysis, Int. J. Hydrogen Energy 29 (2004) 1459–1469.

[11] A. Morozov, Comparative Analysis of Hydrogen Production Methods with Nuclear Reactors, Interlaken, Switzerland, 20-26 September 2008 Paper No. 237.

[12] D.A.J. Rand, R.M. Dell, Hydrogen Energy: Challenges and Prospects, RSC Publishing, Cambridge, 2007. ISBN-10:085404597X.

[13] L.C. Brown, J.F. Funk, S.K. Showalter, Initial Screening of Thermochemical Water-Splitting Cycles for High Efficiency Generation of Hydrogen Fuels Using Nuclear Power, General Atomics, 1999 report number GA-A23373.

[14] J.E. Funk, R.M. Reinstrom, Energy requirements in the production of hydrogen from water, Ind. Eng. Chem. Process. 5 (1966) 336–342.

[15] R. Liberatore, A. Ceroli, M. Lanchi, A. Spadoni, P. Tarquini, Experimental vapour-liquid equilibrium data of HI-H_2O-I_2 mixtures for hydrogen production by Sulphur-Iodine thermochemical cycle, Int. J. Hydrogen Energy 33 (2008) 4283–4290.

[16] A. Singhania, V.V. Krishnan, A.N. Bhaskarwar, B. Bhargava, D. Parvatalu, S. Banerjee, Hydrogen production from the decomposition of hydrogen iodide over nanosized nickel-oxide-zirconia catalysts prepared by solution-combustion techniques, Catal. Commun. 93 (2017) 5–9.

[17] S. Kasahara, J. Iwatsuki, H. Takegami, N. Tanaka, H. Noguchi, Y. Kamiji, K. Onuki, S. Kubo, Current R&D status of thermochemical water splitting iodine-sulfur process in Japan Atomic Energy Agency, Int. J. Hydrogen Energy 42 (2017) 13477–13485.

[18] Z. Ying, X. Zheng, Y. Zhang, G. Cui, Kinetic analysis of Bunsen reaction with HI existence in the thermochemical sulfur–iodine cycle for hydrogen production, Appl. Therm. Eng. 129 (2018) 41–49.

[19] N. Goswami, A. Bose, N. Das, S.N. Achary, A.K. Sahu, V. Karki, R.C. Bindal, S. Kar, DDR zeolite membrane reactor for enhanced HI decomposition in IS thermochemical process, Int. J. Hydrogen Energy 42 (2017) 10867–10879.

[20] L.C. Brown, R. Buckingham, G.E. Besenbruch, B. Wong, G. Polansky, P. Pickard, Engineering Materials Requirements Assessment for the S-I Thermochemical Cycle. GA-A24902, 2005. January 2005, https://fusion.gat.com/pubs-ext/AnnSemiannETC/A24902.pdf (downloaded on. (Accessed 24 May 2019).

[21] B. Belaissaoui, R. Thery, X.M. Meyer, M. Meyer, V. Gerbaud, X. Joulia, Vapour reactive distillation process for hydrogen production by HI decomposition from HI-I_2-H_2O solutions, Chem. Eng. Process 47 (2008) 396–407.

[22] Arifal, G.J. Hwang, K. Onuki, Electro-electrodialysis of hydriodic acid using the cation exchange membrane cross-linked by accelerated electron radiation, J. Membr. Sci. 210 (2002) 39–44.

[23] R. Taylor, R. Krishna, Modelling reactive distillation, Chem. Eng. Sci. 55 (2000) 5183–5229.

[24] M. Roth, K.F. Knoche, Thermochemical water splitting through direct HI-decomposition from H_2O/HI/I_2 solutions, Int. J. Hydrogen Energy 14 (1989) 545–549.

[25] S. Goldstein, J.M. Borgard, X. Vitart, Upper bound and best estimate of the efficiency of the iodine sulphur cycle, Int. J. Hydrogen Energy 30 (2005) 619–626.

[26] J.E. Murphy IV, J.P. O'Connell, A properties model of the HI-I_2-H_2O-H_2 system in the sulfur-iodine cycle for hydrogen manufacture, Fluid Phase Equilib. 288 (2010) 99–110.

[27] S. Mandal, A.K. Jana, A comparative performance of thermodynamic models for a quaternary (HI-H_2O-I_2-H_2) HIx system: experimental verification, Int. J. Hydrogen Energy 41 (2016) 13350–13358.

[28] S. Banerjee, A.K. Jana, High gain observer based extended generic model control with application to a reactive distillation column, J. Process Control 24 (2014) 235–248.

[29] J.E. Murphy IV, J.P. O'Connell, Process simulations of HI decomposition via reactive distillation in the sulfure-iodine cycle for hydrogen manufacture, Int. J. Hydrogen Energy 37 (2012) 4002–4011.

[30] J.E. Murphy IV, J.P. O'Connell, Corrigendum to "A properties model of the HI–I_2–H_2O–H_2 system in the sulfur–iodine cycle for hydrogen manufacture" [Fluid Phase Equilibria 288, Fluid Phase Equilib. 293 (2010) (2010) 99–110, 266.

[31] R. C Reid, J.M. Prausnitz, B.E. Poling, The Properties of Gases and Liquids, fourth ed., McGraw-Hill Book Company, New York, 1987.

[32] A.K. Jana, Chemical Process Modelling and Computer Simulation, third ed., PHI Learning, Delhi, 2018.

[33] A.K. Jana, Process Simulation and Control Using Aspen^{TM}, second ed., PHI Learning, Delhi, 2012.